Picosecond Relaxation Processes in Liquids

Geraldine A. Kenney-Wallace

Phil. Trans. R. Soc. Lond. A 1980 **298**, 309-319
doi: 10.1098/rsta.1980.0256

Phil. Trans. R. Soc. Lond. A **299**, 309–319 (1980)
Printed in Great Britain

Picosecond relaxation processes in liquids

By Geraldine A. Kenney-Wallace
Department of Chemistry, Lash Miller Chemical Laboratories, University of Toronto,
80 St George Street, Toronto, Ontario M5S 1A1, Canada

Recently there have been a number of important experimental and theoretical developments that focus on the dynamics of rotational and vibrational relaxation processes of molecules in liquids. This marks the emergence of a microscopic description of the forces that govern the structure of fluids. Ultra-short laser pulses permit us to observe directly the consequences of these molecular interactions by probing several causally related phenomena, namely electron localization, fluorescence depolarization and optical Kerr rotation in polar liquids. I present recent results from the picosecond laser spectroscopy of relaxation processes in liquids, and discuss their implications in terms of the influence of the molecular motion on reaction dynamics in liquids in general and on electron transfer processes specifically.

1. Introduction

In the past few years we have witnessed exciting developments in ultra-short laser pulses that have stimulated considerable activity in a diverse range of research areas, from nonlinear optics to biophysics (Shank *et al.* 1978; Bradley 1978). Quite independently during this period, important experimental and theoretical advances have also been made concerning the dynamics of rotational and vibrational relaxation processes in liquids (Kivelson 1977; Hynes *et al.* 1978; Oxtoby 1978). This parallelism is not entirely coincidental because picosecond laser spectroscopy, where the probe pulses and the phenomena share the same temporal domain, is a window on molecular dynamics in liquids; it thus offers direct access to a density régime where the intermolecular forces are a predominant factor. The underlying theme of this paper is that picosecond and femotsecond laser spectroscopy will lead ultimately to a quantitative understanding of chemical reaction dynamics in liquids. However, in order to predict the role played by the dynamical molecular structure of the liquid in the outcome of chemical reactions, we first need to investigate the molecular dynamics in *unreactive* systems and study the influence of local liquid structure and short-range dynamical correlations on molecular motion.

In this paper I first examine rotational relaxation processes in liquids from several different perspectives, namely the role of long-range dipolar relaxation and molecular reorientation during electron localization and solvation in polar liquids, the influence of intermolecular interactions on the rotation of a molecule in the same class of liquids, and the influence of a strong local (optical) field on the reorientational dynamics of molecules. I then briefly describe the influence of molecular motions on the outcome of a chemical event that takes place in that liquid, namely electron transfer. In most laser-induced chemistry, there is an intrinsic competition between relaxation processes and reactive events, and thus the details of this reaction have a particular relevance to a wider range of problems in chemical physics such as photoionization and photodissociation, electron trapping, electron transfer and exciton migration, recombination processes, and the formation of charge-transfer complexes and exciplexes.

2. Electron localization and molecular dynamics in liquids

The dynamics of electron relaxation and polaron formation are the subject of current investigation in semiconductors, amorphous solids, and in F centres in alkali halide crystals (Williams *et al.* 1978). In fact, the F_A II colour centres now represent a new class of picosecond lasers (Mollenauer *et al.* 1978). In liquids, too, strong short-range electron–medium interactions can often lead to electron localization whereby the electron becomes trapped in a cluster of molecules (Kenney-Wallace & Jonah 1977, 1980). These short-lived (not more than 1 μs), but nevertheless chemically discrete, species present the simplest case in which to explore the influence of the molecular dynamics of the liquid on the clustering process and on subsequent photodetachment and electron transfer processes. The implications of the results, however, have far-reaching consequences in the more practical areas of dielectric breakdown and laser-induced nucleation phenomena.

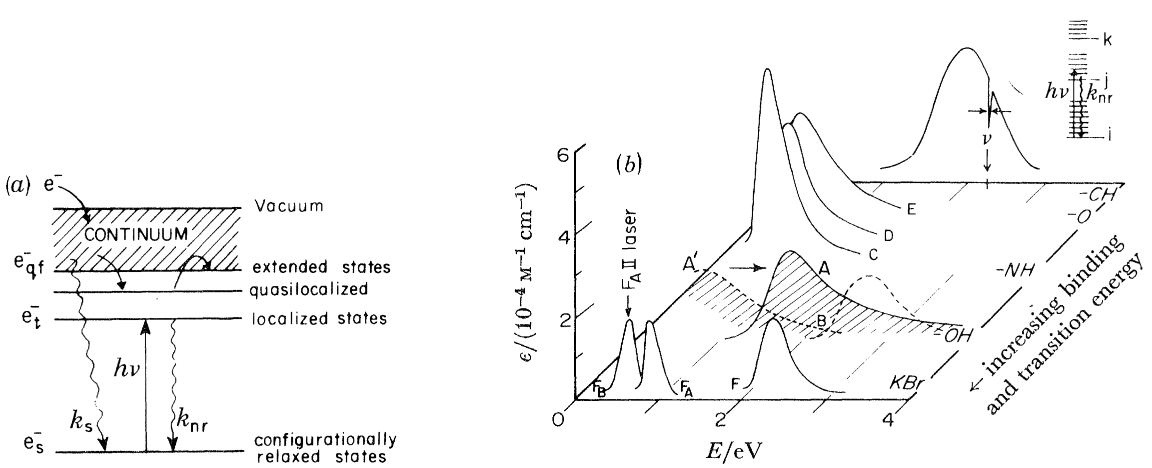

Figure 1. Excess electronic states in liquids. (*a*) A diagram of electronic energy levels illustrating transitions between extended (e^-_{qf}) and localized (e^-_t, e^-_s) states. (*b*) Optical spectra and absorption coefficients of electrons in *n*-alcohols at picosecond (A′) and nanosecond (A) times, diols (B), amines (C), ethers (D), alkanes (E) and as colour centres (F, F_A). The colour centre laser emission in KBr is shown as F_B.

I shall briefly review the theoretical framework for these electron studies. Figure 1*a* is a diagram of the electronic energy levels attributed to these excess electron states in liquids (Jortner & Gaathon 1977; Kenney-Wallace 1978). Upon ejection into a liquid, the electron is initially in an extended state and scatters through the fluid with a high mobility ($1 < \mu < 10^3\ \mathrm{cm^2\,V^{-1}\,s^{-1}}$) that depends upon the mean free path for momentum transfer and thus upon the strength of the electron–molecule scattering potential (Davis & Brown 1975). When localization occurs it can be to a quasi-localized state, lying just below the mobility edge (V_0) and within a thermal fluctuation of the continuum state, or to a truly localized state e^-_s of 1–2 eV binding energy, where the electron is confined in a configurationally relaxed cluster of polarized molecules in the liquid. In the ground electronic state, e^-_s exhibits intense broad absorption bands which appear in spectral groupings according to the short-range electron–molecule interactions and the molecular structure of the liquid. Figure 1*b* is an ensemble of these absorption spectra and shows the wide range of liquids in which electrons can be studied. The position of the optical absorption is indeed a signature of the trapping potential experienced by the electron. The $E\lambda_{max}$ for e^-_s in the series methanol to decanol falls within 1.80 ± 0.1 eV.

Thus by recording the temporal evolution of the e_s^- absorption in a class of dipolar liquids, which display identical stable e_s^- spectra but varying molecular dynamics, we hope to observe directly in picosecond spectroscopy the transition between the extended and localized states, accompanied by the polarization and reorganization of the molecules about the electron. I also report here isotope studies of the dynamics of a unique laser-induced electron transfer from excited states of e_s^- in liquid alcohols, observed in 'hole-burning' experiments.

3. Experimental arrangements

A number of different experimental approaches may be followed in order to investigate molecular motion in liquids with ultra-short laser pulses. These include transient absorption and emission spectroscopy, fluorescence depolarization, conjugate wave formation, transient grating formation and optical Kerr spectroscopy. Information is thus obtained on the vibrational population relaxation (T_1) and dephasing (T_2) times, the rotational relaxation, translational diffusion and the coupling of one mode of motion to another in the same molecule or to those of the bath molecules.

The results reported here have been obtained through several of these picosecond pump–probe techniques. Electron localization has been studied in picosecond absorption spectroscopy, via multi-photon photoionization of an impurity molecule in the liquid with the harmonics from mode-locked solid state lasers and via direct ionization of the liquid with a picosecond pulsed electron beam. In both techniques we employ a picosecond continuum to probe the subsequent transient spectra and kinetics, and the temporal resolution of the measurement is derived from a precise knowledge of the difference in optical pathlengths travelled by the pump and probe pulses. While the powers available, not more than 10 GW in a single 6 ps pulse from a Nd glass oscillator–amplifier system, are necessary in experiments requiring sequential nonlinear interactions, multi-photon photoexcitation or investigating field-induced (optical Kerr) phenomena, the system's typical 10^{-2} Hz repetition rate prevents reliable observations being made on very small signals. The stroboscopic pulsed e-beam facility (Jonah 1975) can be operated at not more than 60 Hz and transient absorptions are interrogated either with a picosecond Čerenkov continuum or a laser, pulsed synchronously with the electron beam. Signal averaging and sampling techniques permit very weak absorption signals to be extracted from the data.

A third, and possibly the most flexible, technique for the future employs synchronously pumped, argon-ion jet stream dye lasers. The principles of operation that have led to a new era of ultra-short dye laser pulses are discussed in detail elsewhere in this volume by Adams *et al.* and Ippen. We employ an actively mode-locked (41 MHz) argon-ion laser, which synchronously pumps a jet stream dye laser in a folded, three-mirror, extended cavity. With an average power of 900 mW and argon laser pulses of $\leqslant$ 120 ps duration, we have obtained routinely dye laser pulses of less than 1 ps duration, *ca.* 1 nJ in energy and extremely stable over long periods of time. Autocorrelation traces show that the pulse shape is excellent and does not exhibit long tails. This is a crucial point, since the advantages of having subpicosecond pulses to study chemical dynamics become questionable if there is substantial intensity in the wings of the pulses, which, extending into many picoseconds, blur the temporal evolution of the signal. We have amplified these dye laser pulses, in the spirit of Ippen & Shank, with a series of dye amplifiers pumped at 10 Hz by the frequency-doubled output of a Nd:YAG laser. With an expected gain of about 10^6, the laser pulses will be of not more than gigawatt powers, comparable with those from the Nd glass system, but with the important additional advantages of shorter pulses, a 10 Hz repetition rate and wavelength tunability across visible wavelengths achieved by direct pumping or by resonant energy transfer schemes (Kenney-Wallace *et al.* 1975; Sala *et al.* 1980).

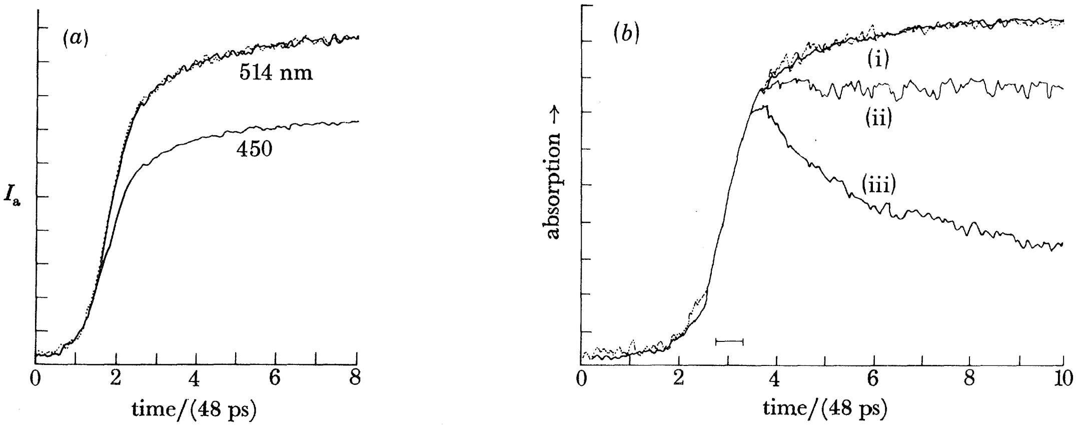

FIGURE 2. Dynamics of electron solvation. (*a*) Absorption in 1-decanol at 450 and 514 nm. (*b*) Absorption in 2-decanol at 600 nm. Trace (i) is a superposition of the signals in pure 2-decanol and *t*-butanol. Traces (ii) and (iii) are 2-decanol in *n*-hexane at $\langle \rho_d \rangle = 3 \times 10^{20}$ and 3.5×10^{19} cm^{-3}, respectively.

4. RESULTS AND DISCUSSION

(*a*) *Electron localization in pure liquids, n-alcohols*

When picosecond spectroscopy is employed to monitor the evolution of these e_s^- spectra in alcohols from methanol to decanol, in every case the initial spectrum observed at the earliest times (less than 6 ps) appears in the near infrared, represented by A′ in figure 1*b*. This structureless, infrared absorption band rapidly disappears as the visible e_s^- spectrum grows. The absorption signal in the visible is characterized by a fast (less than 6 ps resolution time) and a slow component, the latter growing in over several hundred picoseconds in the long-chain alcohols. Analysis of these exponential signals shows that the kinetics are similar for the time-dependent loss of the i.r. spectrum and the appearance of the visible spectrum represented by the slow component of the signal (Chase & Hunt 1975; Huppert *et al.* 1979). Typical visible absorption signals recorded in 1-decanol (C_{10}) and 2-decanol (2-C_{20}) are shown in figure 2. At wavelengths shorter than λ_{max}, the absorption signals vary in amplitude, but upon normalization they exhibit the same temporal profile shown in figure 2*a* by the dotted line. Therefore we can now discuss the solvation dynamics of e_s^- in terms of the time-dependent absorption signals at visible probe wavelengths. Trace (i) in figure 2*b* is a superposition of the normalized absorption signals in 2-decanol and (dotted) *t*-butanol. Table 1 summarizes the solvation times, τ_s, derived from these absorption data in a series of alcohols and compares them with the rotational relaxation times τ_2 of the alcohol monomers independently obtained from dielectric dispersion measurements (Garg & Smyth 1965). The uncertainty of the data is ± 10 %. The agreement is extremely good and the interpretation of this result is that the dynamics of electron solvation are governed by rotational diffusion to form a cluster of molecules in which the electron becomes stabilized

(Kenney-Wallace & Jonah 1977). However, the strong local field of the electron and its influence on the microscopic liquid structure present two further points of concern to which I shall return in discussing the Kerr effect.

Table 1 also includes liquid properties such as viscosity, η, orientational polarizability, α_0, and average dipole density, $\langle\rho_d\rangle$, defined as OH dipole/cm³. When these solvation data are plotted in a hydrodynamic-like representation, as in figure 3, based on the Stokes–Einstein–Debye equation (1), a linear relation is observed that also encompasses the measurements of

$$\tau_s^{-1} = \alpha_0 \eta^{-1} (kT/V) \tag{1}$$

τ_2 for rotational relaxation in the absence of the electron in the alcohols. Furthermore, a similar correlation can be seen by using the dielectric relaxation data for 1,2,3-tribromopropane (Roy *et al.* 1976) for which no solvated electron states are known. Clearly the response of the liquid to the sudden presence of the electron during solvation appears 'hydrodynamic' and an intrinsic function of the liquid dynamics.

TABLE 1. ELECTRON SOLVATION TIMES, τ_s, IN ALCOHOLS AT 298 K

C_n	C_1	C_2	C_3	C_4	C_5	C_8	C_{10}
η/cP†	0.55	1.10	2.00	2.60	3.35	8.95	14.1
$\langle\rho_d\rangle/(10^{21}\ \mathrm{cm}^{-3})$	14.8	10.2	8.0	6.5	5.5	3.8	3.1
τ_s/ps	10	18	25	30	34	45	50
τ_2/ps	12	20	22	27	28	39	48

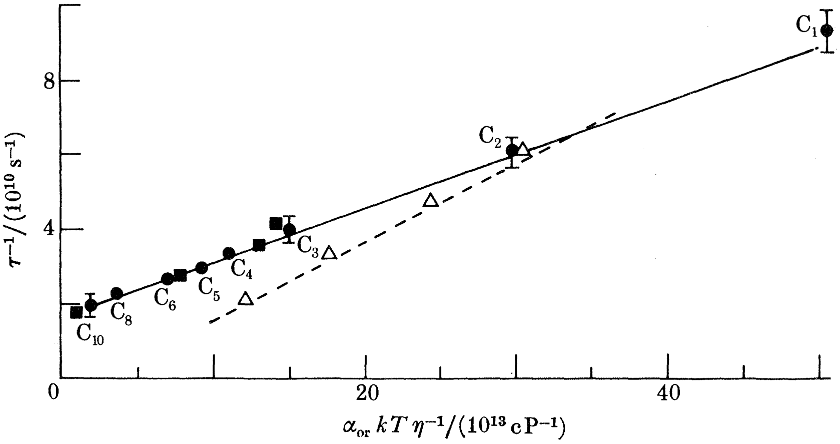

FIGURE 3. Hydrodynamic representation of solvation data in alcohols. (●) 1-alcohols, (■) 2-alcohols, (△) 1, 2, 3-tribromopropane. See text for discussion.

Note that τ_s increases with decreasing $\langle\rho_d\rangle$ and increasing η. However, we observe that electron solvation in glycol (B in figure 1*b*) occurs within the time resolution of the apparatus (less than 10 ps) despite the high $\langle\rho_d\rangle$, 2.15×10^{22}, and high viscosity, η = 20 cP.† In the context of a liquid structure approach, however, the last result is not surprising, for two reasons. First, the binding and transition energy of e_s^- in glycol are among the highest known for an excess electron state, and we can envisage the electron trapped within a chelate-like configuration involving two (or more) molecules as the inner part of the cluster. Such hydrogen-bonded

---

† 1 cP = 1 mPa s.

structures certainly coexist in dynamic equilibrium in the liquid. Thus, during electron solvation, the availability of this pre-existing trapping site and the high $\langle\rho_d\rangle$ would predict a solvation time in the time domain more representative of relaxation processes in water where $\langle\rho_d\rangle$ is 3.33×10^{22} and τ_s is probably *ca.* 10^{-12} s (Rentzepis *et al.* 1973; Chase & Hunt 1975; Kenney-Wallace 1978).

(*b*) *Electron localization in dilute fluids*

When the alcohols are diluted to a very low number density $\langle\rho_d\rangle$ in an alkane of comparable chain length, rather different kinetics are observed. Figure 2*b* summarizes the results. Three regions of distinct kinetic and spectral behaviour can be delineated for every alcohol: alkane system as a function of $\langle\rho_d\rangle$. At very low $\langle\rho_d\rangle$, a weak i.r. absorption is observed which rapidly decays within 200 ps. The amplitude and decay of the signal in trace (iii) is identical to that in pure alkane until a critical value of $\langle\rho_d\rangle$ is reached, above which, as $\langle\rho_d\rangle$ increases, the decay of the signal becomes slower and eventually attains a plateau, as in trace (ii). No spectral shifts can be detected up to this stage. For 2-decanol in *n*-hexane the threshold value of $\langle\rho_d\rangle$ is 3×10^{19} and the plateau is reached at 3.5×10^{20}. For *t*-butanol, the threshold and plateau occur at 1.5×10^{20} and 1.4×10^{21}, respectively, even though the dynamics of e_s^- solvation in pure *t*-butanol and 2-decanol are the *same*, $\tau_s = 54$ ps, in trace (i). Further increases in alcohol density lead to a growth in the picosecond absorption signal, characteristic of the pure fluid e_s^- dynamics, and by $\langle\rho_d\rangle \approx 7 \times 10^{20}$, the spectral shifts from i.r. to the visible simulate those recorded in the pure 2-decanol. Similar absorption–dipole density profiles are seen for all the alcohol: alkane systems studied to date (Kenney-Wallace *et al.* 1977, 1980) and are a quantitative optical analogue of electron mobility measurements in mixed systems (Baxendale 1977).

A compelling interpretation of these results is that, through electron localization, we can distinguish at least three density régimes in these alcohol alkane systems, each of which may be dominated by different local structures in the fluid. To pursue this point, we investigated the internal mobility of the various carbon atoms in the alkyl chains by means of ^{13}C Fourier transform n.m.r. (Ling *et al.* 1978). At low alcohol densities, significant increases were observed for the spin lattice relaxation time (T_2) of the carbon atom C(1) attached to the OH group, implying far less restricted internal motion and hence faster (picosecond) rotational correlation times. For example, in *n*-butanol: cyclohexane the T_1 values for C(1) increased from 4.29 to only 5.94 s upon dilution over the range $\langle\rho_d\rangle = 13$ to 3×10^{20} cm^{-3} but dramatically increased to 16.32 s by 1.6×10^{19} cm^{-3}, a value just below the threshold $\langle\rho_d\rangle$ observed in picosecond spectroscopy studies of e_s^- in the same system. The substantial variations in T_1 in C(1) in the very low $\langle\rho_d\rangle$ alcohol: alkane systems are attributed to the breaking up of the hydrogen-bonded alcohol clusters that dominate the local liquid structure in a mixture of high alcohol density. At very low $\langle\rho_d\rangle$, therefore, the alcohol molecules are essentially monomeric.

We are now able to place a more quantitative interpretation on the results in figure 2*b*, by comparing the n.m.r. with the optical data. In pure alkane and at very low $\langle\rho_d\rangle$, the excess electron scatters in the alkane, the weak i.r. absorption being assigned to a quasi-localized state, until ion recombination occurs. Not until a threshold $\langle\rho_d\rangle$ is reached, signifying the onset of alcohol clustering, is there an alternative to neutralization, namely capture by an alcohol cluster of say two or three molecules to form a localized electron state. Furthermore, by studying e_s^- solvation in a given alcohol diluted in a range of alkanes with varying shape and structure, the critical $\langle\rho_d\rangle$ can be qualitatively predicted by knowing the relative magnitude of the solute–solvent interactions before electron ejection.

In summary, the electron solvation data in dilute fluids indicate that (*a*) a critical density of alcohol molecules is required before electron trapping in alcohols can occur, and (*b*) this density régime corresponds to the onset of changes in the local liquid structure brought about by clustering of the alcohol molecules before electron ejection. Subsequent increases in the number density of alcohol molecules continue to affect the local structure such that the size and distribution of clusters increases until the electrons are localized and solvated in molecular structures whose dynamical responses simulate those of the pure fluid.

We conclude that electron solvation in these dilute fluids reveals microscopic details of the liquid that are masked by the apparent 'hydrodynamic' behaviour of the pure system in figure 3. This statement will be echoed by the rotational relaxation data on dyes presented below.

(*c*) *Fluorescence depolarization studies of dye molecules*

The influence of intermolecular interactions on the rotation relaxation of molecules embedded in different solvents can be investigated by fluorescence depolarization or transient-induced dichroism in picosecond laser spectroscopy (Porter *et al.* 1977; Fleming *et al.* 1977; Eisenthal 1977). Of major interest is whether or not orientational relaxation of molecules can be described by the Stokes–Einstein–Debye relationship, $\tau_{\mathrm{or}} = \eta V(kT)^{-1}$, which assumes hydrodynamic or 'stick' boundary conditions. Recent microscopical theories of rotational diffusion (Kivelson 1977; Hynes *et al.* 1978) predict significant deviations from hydrodynamic behaviour and focus on the nature and the extent of the coupling of the rotational and translational motions of the molecule under observation to those of its neighbours. These 'slip' boundary conditions can be derived from picosecond spectroscopy studies but the interpretation of the data is a particularly sensitive function of the shape of the molecules and solute–solvent interactions.

We have recently studied the fluorescence depolarization of several xanthene dyes in the same range of alcohols employed in the electron solvation studies, in an endeavour to observe the predicted saturation in the linear relation between τ_{or} and η (Hynes *et al.* 1978), and to provide further evidence for the importance of short range solvent structure on molecular motion. Some results from our study on Rhodamine 6G in *n*-alcohols (Rice & Kenney-Wallace 1980) are shown in figure 4 in comparison with earlier work (Eisenthal 1977). Also included are data for eosin-y and fluorescein, all at 298 K. Full details of this work will appear elsewhere but the salient points for this discussion are as follows. First, as noted earlier by Eisenthal and coworkers, the rotational reorientation time of Rhodamine 6G in a series of alcohols up to *ca.* 10 cP (1 Pa s) appears to follow the hydrodynamic predictions. However, at higher viscosities, our data show that there is indeed a saturation in the predicted τ_{or} value. Apparently the rotational reorientation times are much *faster* than expected on the basis of the viscosity of these mixtures of ethylene glycol and glycerol. When the temperature dependence of the rotation relaxation of Rhodamine 6G in glycerol is compared with the temperature dependence of the viscosities of pure glycerol, the latter reveals a slope that is almost an order of magnitude larger than the former.

We interpret these data as a clear demonstration that once again it is the details of the short-range solvent structure and local intermolecular interactions that govern the dynamical behaviour of Rhodamine 6G in these high-viscosity systems.

As with e_s^-, the dye molecule appears to be located in a solvent cage arising from the multiple-hydrogen bonding sites on these high $\langle\rho_d\rangle$ liquids. Once in this environment, changes to the macroscopic properties of the fluid have little effect on the local solute–solvent interactions and the magnitude of the torque experienced by the dye molecule. The hydrodynamic volumes calculated from plots similar to figures 3 and 4 yield effective radii for the rotating species but, as noted by Fleming *et al.* (1977), there is a certain ambiguity in deciding whether it is the boundary condition or the solvation volume – or both – that is changing as one studies reorientation dynamics of a given molecule in a range of liquids. We are presently pursuing these fluorescence depolarization studies in less complex fluids, to elucidate the quantitative details of the short-range dynamical correlations, which are the corner-stone of the microscopic theories of rotational diffusion.

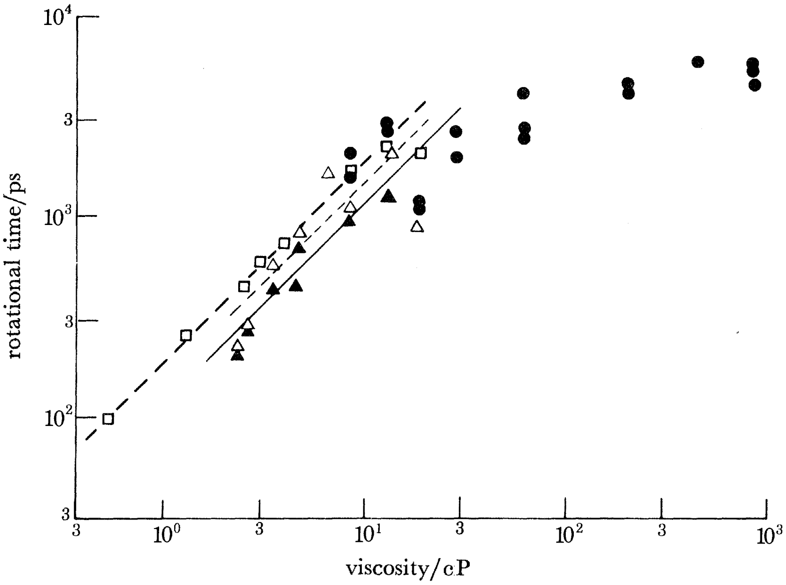

FIGURE 4. Rotational relaxation time of (●) Rhodamine 6G, (▲) eosin-y, (△) fluorescein in alcohols, as a function of viscosity; (□) Rhodamine 6G (Eisenthal 1977).

(*d*) *Dynamics of the optical Kerr effect*

The optical Kerr effect has been employed extensively as an ultra-fast optical gate in picosecond laser spectroscopy. The time-dependence of the transmission of the gate is proportional to $\delta_n(t)$ which is expressed as (Sala & Richardson 1975):

$$\delta_n(t) = (n_2/\tau)\int_{-\infty}^{t} E^{-2}\,(t')\,[\exp\,-(t-t')/\tau]\,\mathrm{d}t', \qquad (2)$$

where $n(t)$ is the sum of both the normal and nonlinear refractive indices at an applied laser (optical) field, E and τ is the relaxation time of the medium. Time-reversal arguments would claim that the response time of the system in aligning to the applied field of the picosecond laser pulse will be identical to the rotational (Debye) relaxation time of the system as it returns to a spatially isotropic distribution when the field is off. However, arguments whose roots lie in the recent development of the microscopic details of molecular dynamics and intermolecular potentials in liquids lead us to expect an asymmetry in the rise and decay transients of the optical Kerr effect. We are thus currently investigating the full dynamics of the optical Kerr effect to describe the influences of strong local fields on molecular motion, an area clearly pertinent to studies of electron solvation. The answers to these questions are also of fundamental importance to our basic understanding of molecular dynamics in fluids, and to future modelling of the interaction of intense transient laser fields with molecules at number densities where collective effects are expected to dominate the intermolecular interactions.

5. Laser-induced electron transfer

In liquids and in supercritical vapours (Jortner & Gaathon 1977), the spectral line width of the e_s^- absorption is very broad, typically 1 eV, but unlike F centres, no radiative processes have been observed. Laser saturation or 'hole-burning' experiments have been performed (Kenney-Wallace & Walker 1971; Huppert & Rentzepis 1976; Kenney-Wallace & Sarantidis 1978) to investigate the spectral homogeneity of the band and the nature and lifetime of the electronically excited state (s) of e_s^- in water, liquid amines and alcohols. All the evidence points towards a homogeneously broadened, bound–bound transition with excited state lifetimes in the picosecond régime. If spectral broadening is largely due to strong electron–phonon coupling (Ulstrup & Jortner 1975; Banerjee & Simons 1978; Funabashi *et al.* 1978), then photodetachment and electron transfer should be sensitive to these interactions too.

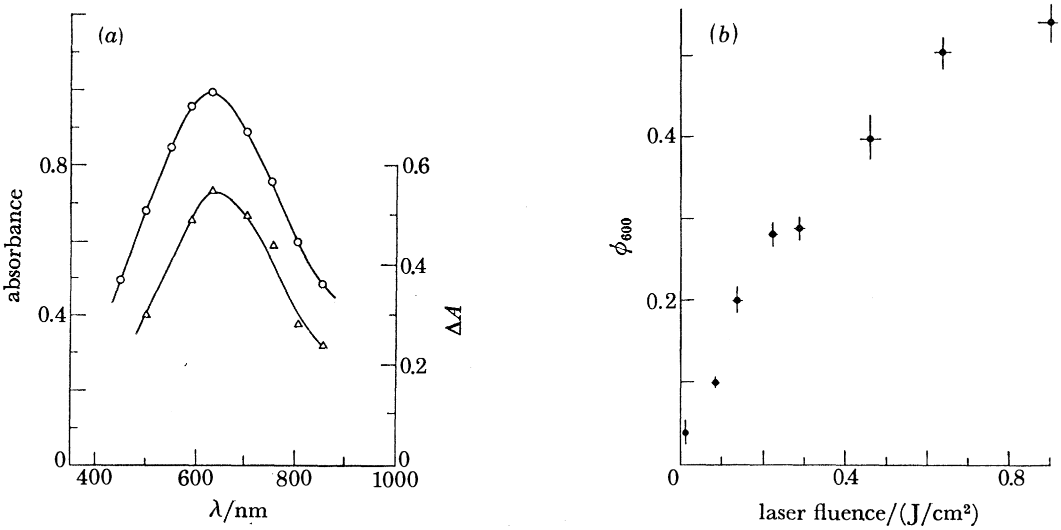

FIGURE 5. Laser photobleaching of e_s^- in methanol. (*a*) e_s^- spectrum (○) before arrival of laser saturation pulse at 694 nm (△), after optical saturation. (*b*) The dependence of electron loss ϕ_{600} on laser fluence (J cm^{-2}) in the same system.

In hole-burning experiments on e_s^- in methanol (illustrated schematically in figure 1*b*), it was also observed that at high incident laser intensities, full recovery of the ground state population did not occur (Bromberg & Thomas 1975; Kenney-Wallace & Sarantidis 1978). Our evidence from many alcohols further indicated that at these laser intensities the permanent loss of intensity displayed the same wavelength (η) dependence as the absorption cross section. This is shown in figure 5*a* for e_s^- in methanol subjected to a laser bleaching pulse at 694 nm. Furthermore, the normalized electron loss, ϕ_λ, was a sensitive function of the laser intensity, as plotted in figure 5*b* against laser fluence (J cm^{-2}) at 694 nm. At intensities greater than 0.6 J cm^{-2} there appeared to be little further increase in ϕ_λ for e_s^-, whereas in optically equivalent solutions of dyes such as cryptocyanine or DDI in methanol, total transient bleaching was observed with ground state recovery times of 38 and 10 ps, respectively, in agreement with literature values (Mourou *et al.* 1973). Clearly there is a competition between rapid vibronic relaxation of e_s^{-*} and laser-induced chemical reaction from the excited state, leading to loss of e_s^-.

When the laser saturation experiments were carried out on e_s^- in a series of deuterated alcohols, isotope effects were observed that showed conclusively that the chemical channel was correlated to the vibration of the –OH bond. For example, at an incident laser intensity of 0.35 J cm^{-2}, ϕ_{600} was 0.30 in CH_3OH, 0.32 in CD_3OH but 0.04 in CH_3OD. The magnitude of the isotope effect also depended on the laser intensity. We conclude that although the CH and CD vibrations of the molecules in the cluster must contribute to the fast radiationless relaxation of e_s^{-*}, it is the OH vibration that leads to photochemistry. Strong coupling of the high frequency intramolecular vibrational modes of the –OH bond and the electronic states of the electron apparently lead to bond dissociation and electron attachment under high laser intensities:

$$e_s^- + h\nu(1.78) \rightarrow e^{-*} \rightarrow RO^- + H. \tag{3}$$

Deuteration has presumably weakened the coupling or led to unfavourable Franck–Condon factors (Ulstrup & Jortner 1975). The potential surface for the above dissociative reaction must cross the excited state surface from which e_s^{-*} normally relaxes to the ground state, and in ROH clusters under high laser intensities, significant numbers of e_s^- have access to this channel.

There are still several aspects of this *intracluster* laser-induced electron transfer process that remain to be unravelled by means of tunable picosecond laser spectroscopy. Nevertheless, these data offer a novel example of the competition between relaxation and reaction, and illustrate the potential of ultra-short laser pulses to probe the dynamics of chemical reactions in liquids.

The author gratefully acknowledges the contributions of Dr C. D. Jonah (A.N.L.) and Dr B. A. Garetz, Dr S. A. Rice, Mr G. E. Hall, Mr K. Sarantidis and Miss L. M. Hunt to this research, and the financial support from the Natural Science and Engineering Research Council of Canada and the Petroleum Research Fund, administered by the American Chemical Society. The author is an Alfred P. Sloan Foundation Fellow.

REFERENCES (Kenney-Wallace)

Banerjee, A. & Simons, J. 1978 *J. chem. Phys.* **68**, 415–432.
Baxendale, J. H. 1977 *Can. J. Chem.* **55**, 1996–2002.
Bradley, D. J. 1978 *J. phys. Chem.* **82**, 2259–2268.
Bromberg, A. & Thomas, J. K. 1975 *J. chem. Phys.* **63**, 2124–2130.
Chase, W. J. & Hunt, J. W. 1975 *J. phys. Chem.* **79**, 2835–2845.
Davis, H. T. & Brown, R. G. 1975 *Adv. chem. Phys.* **31**, 329–464.
Eisenthal, K. 1977 *A. Rev. phys. Chem.* **28**, 207–232.
Fleming, G. R., Knight, A. E., Morriss, J. M., Robbins, R. J. & Robinson, G. W. 1977 *Chem. Phys. Lett.* **51**, 402; and references therein.
Funabashi, K., Carmichael, I. & Hamill, W. H. 1978 *J. chem. Phys.* **69**, 2652–2656.
Garg, S. K. & Smyth, C. P. 1965 *J. phys. Chem.* **69**, 1294–1301.
Huppert, D., Rentzepis, P. M. & Kenney-Wallace, G. A. 1979 In preparation.
Huppert, D. & Rentzepis, P. M. 1976 *J. chem. Phys.* **64**, 191–196; and references therein.
Hynes, J. T., Kapral, R. & Weinberg, M. 1978 *J. chem. Phys.* **69**, 2725–2733; and referenecs therein.
Jonah, C. D. 1975 *Rev. scient. Instrum.* **46**, 62–66.
Jortner, J. & Gaathon, A. 1977 *Can. J. Chem.* **55**, 1801–1819.
Kenney-Wallace, G. A. 1978 *Acct. chem. Res.* **11**, 433–439.
Kenney-Wallace, G. A., Flint, J. H. & Wallace, S. C. 1975 *Chem. Phys. Lett.* **32**, 71.

Kenney-Wallace, G. A. & Walker, D. C. 1971 *J. chem. Phys.* **55**, 447–451.
Kenney-Wallace, G. A. & Jonah, C. D. 1977 *Chem. Phys. Lett.* **47**, 362–366.
Kenney-Wallace, G. A. & Sarantidis, K. 1978 *Chem. Phys. Lett.* **53**, 495–498.
Kenney-Wallace, G. A. & Jonah, C. D. 1980 *Chem. Phys. Lett.* (In the press.)
Kivelson, D. 1977 *Faraday Symp. chem. Soc.* **11**, 7–25.
Ling, R., Kenney-Wallace, G. A. & Reynolds, W. F. 1978 *Chem. Phys. Lett.* **54**, 81–84.
Mollenauer, L. F., Bloom, D. & Del Gaudio, A. 1978 *Optics Lett.* **3**, 48–50.
Mourou, G., Drouin, B., Bergeron, M. & Denariez-Roberge, M. 1973 *IEEE J. Quantum Electron.* **QE-9**, 745.
Namiki, A., Nakashima, N., Yoshihara, K., Ito, Y. & Higashimura, T. 1978 *J. Phys. Chem.*, **82**, 1901–1907.
Oxtoby, D. 1980 *Adv. chem. Phys.* **47**. (In the press.)
Porter, G., Sadkowski, P. J. & Tredwell, C. J. 1977 *Chem. Phys. Lett.* **49**, 416.
Rentzepis, P. M., Jones, R. P. & Jortner, J. 1973 *J. chem. Phys.* **59**, 766–773.
Rice, S. A. & Kenney-Wallace, G. A. 1980 *Chem. Phys.* **47**, 161–170.
Roy, S. K., Gupta, K. S., Ghatak, A. & Das, A. 1976 *J. chem. Phys.* **65**, 3595–3598.
Sala, K. & Richardson, M. C. 1975 *Phys. Rev.* A **12**, 1036–1047.
Sala, K., Kenney-Wallace, G. A. & Hall, G. E. 1980 *IEEE J. Quantum Electron.* (In the press.)
Shank, C. V., Ippen, E. P. & Shapiro, S. L. (eds) 1978 *Picosecond Phenomena*. New York: Springer-Verlag.
Ulstrup, J. & Jortner, J. 1975 *J. chem. Phys.* **63**, 4358–4368.
Williams, R. T., Bradford, J. N. & Faust, W. L. 1978 *Phys. Rev.* B **18**, 7038